Available online www.jsaer.com

***Journal of Scientific and Engineering Research*, 2023, 10(11):18-28**

Research Article

ISSN: 2394-2630
CODEN(USA): JSERBR

A Novel Method for Forecasting COVID-19 based on Visibility Graph and Link Prediction

Hua Xu

Department of Mathematics, Nanjing Normal University Taizhou College, Taizhou 225300, Jiangsu, China
*Email: xuhua1590526@163.com

Abstract COVID-19 pandemic badly damaged people's health and economy. Its forecasting attracted great attention of scientists and researchers around the globe. A novel COVID-19 prediction model is proposed based on visibility algorithm and link prediction method. The basic idea of model construction is to transform the COVID-19 infection data into a complex network using visibility algorithm, and determine the node similarity in the network with link prediction method. On the basis of analyzing the similarity of nodes, two kinds of initial prediction methods based on the trend weighting of historical nodes and the trend weighting of similar nodes were proposed. Considering the principle of new information priority in the prediction process, the two kinds of initial prediction models were weighted together by defining the distance weight of time variable. Then, a COVID-19 prediction model based on visibility algorithm and link prediction is constructed. The total number of COVID-19 infections and daily new infections in four provinces of Pakistan were used for prediction analysis. The results show that the prediction model constructed in this paper has high prediction accuracy, and the prediction accuracy of the model can be improved by setting the number of similar nodes in the model.

Keywords Visibility Algorithm; Link Prediction; Complex Network; Prediction Model

1. Introduction

The coronavirus disease 2019, abbreviated as COVID-19, is a viral disease caused by the severe acute respiratory syndrome coronavirus 2 (SARS-CoV-2) that produces fever, cough, and dyspnea, as well as muscle pains and chest issues in a minority of cases [1–2]. The virus is primarily transmitted to humans through respiratory channels, and the number of patients is asymptomatic or have mild symptoms, but some develop pneumonia or multi-organ insufficiency (the worst of which is lethal acute respiratory distress syndrome (ARDS) [3]. The period from exposure to the appearance of symptoms ranges from 2 to 13 days, with a 5-day average, with the long-range being affected by the disease's relevance with the common cold in its asymptomatic or soft symptomatology aspect [4,5]. After the 13th day of exposure, 25–30 percent of patients weaken and acquire respiratory infection, while 83 percent develop the symptoms of lymphopenia [6]. On the other side, children can also have the condition, albeit they usually have mild symptoms [7,8].

The COVID-19 worldwide epidemic has affected the world significantly. In simply a short time, from limited local transmission in some states, COVID-19 evolved into a multicounty spread and raged in further more than 100 regions across five continents [9]. Millions of people's lives have been disturbed and affected by the COVID-19 epidemic, which has significantly impacted international relations and the economy. The prevention and control of the COVID-19 pandemic are currently receiving more attention. In some nations, such as China and Germany, the pandemic is well under control, but most countries, including the United States and India, still lack comprehensive COVID-19 control measures. Governments in many nations and areas have made the fight

against the COVID-19 pandemic a top priority, and importantly the public health sector has paid extraordinary attention to saving people's lives.

Complex network is a hot research topic in recent years, the main idea is to link between the real part of the system as a complex network, in the form of a network to describe the relationship between the real part of the system, so as to better understand the essence of reality system. With the development of the scale-free network model [10], the small-world network [11], the Newman and Watts network [12], and the random network model [13], complex network is applied in more and more fields, which provides us a new perspective and approaches to the study of the complexity problems. In recent years, complex network theory has flourished in the field of nonlinear time series analysis. The main idea of this method is to investigate the time series by mapping them to the complex networks. Representing the time series through a corresponding complex network, we can then explore the dynamics of the time series from network organization, which is quantified via a number of topological statistics. This paper builds a COVID-19 prediction model based on complex network theory and link prediction method, which involves three major processes. The data of COVID-19 infections are first transformed into a network using a visibility graph. Then the node similarity is calculated using a link prediction method based on a local random walk. Second, based on the examination of node similarity, the initial predictions are created using the neighboring prediction method and the linear approximation method.

The remainder of this paper is organized as follows. Section 2 describes the method used in this paper. Section 3 discusses the effectiveness and superiority of this method in COVID-19 forecast. Section 4 is the summary and brief conclusion of this paper.

2. Material and Methods

The prediction method proposed in this paper consists of three main steps. The data of COVID-19 infections are first transformed into a network using a visibility graph. Then the node similarity is calculated using a link prediction method based on a local random walk. Second, based on the examination of node similarity, the initial predictions are created using the neighboring prediction method and the linear approximation method.

2.1 Visibility graph

A visibility graph is a method to map time series into complex network. As proposed by Lacasa et al (2008) [14], the basic idea is to treat each data point of time series as a network node and to set up an edge between nodes if the "visual condition" is satisfied. The specific mathematical description is as follows: Let $\{x(t_i)\}_{i=1,2,..,N}$ be a time series containing *N* data, and there is an edge between node i and node j if and only if the following visual criteria are met:

$$x(t_k) < x(t_i) + \left[x(t_j) - x(t_i)\right]\frac{t_k - t_i}{t_j - t_k} \quad , \ t_i < t_k < t_j \tag{1}$$

According to the visibility graph algorithm, a time series containing *N* data can be mapped into a network containing *N* nodes. The principle of a visibility graph is simple, and the visibility graph network obtained has connectivity properties such as undirected affine invariance, and limited information loss. It can also effectively distinguish a random sequence from a chaotic sequence. The complexity of the visibility graph algorithm is $O(n^2)$; thus, it needs a lot of computation time in practical application, which restricts its application in practice. To reduce the time complexity of the algorithm, Luque et al (2010) modified the visual criterion as follows [15]:

$$x(t_i), x(t_j) > x(t_k), \text{ for any } t_i < t_k < t_j \tag{2}$$

This algorithm is called the horizontal visibility graph algorithm (HVG). This algorithm not only maintains the related properties of visibility graph algorithm but also carries out theoretical analysis on specific time series. The complexity of the algorithm is $O(n)$, which greatly reduces the computational complexity compared with the visibility graph algorithm and has higher application value.

2.2 Link prediction

The link prediction method based on LRW can be used to find the potential edges in the network. Probability transition matrix P represents the random walk state of nodes. In a network with N nodes, the probability of moving from node i to node j is expressed by P_{ij} and calculated by Eq. (3).

$$P_{ij} = \frac{a_{ij}}{s_i} \tag{3}$$

where $a_{ij} = 1$ if node i is connected with node j, otherwise $a_{ij} = 0$. $k_i$is the degree of node i, i.e., $k_i = \sum_j a_{ij}$. After step t, the probability of reaching other nodes from node i can be represented by $\vec{\pi}_i$,

$$\vec{\pi}_i(t) = P^T \vec{\pi}_i(t-1) \tag{4}$$

where P^T is the transpose of P. Note that in the initial state, i.e., when $t = 0$, the random walkers standing at node i are described by $N \times 1$ line vector, denoted $\vec{\pi}_i(0)$. The ith element of $\vec{\pi}_i(0)$ is equal to 1, other elements are equal to 0.

Assume that the initial resource distribution of each node is $\frac{k_i}{2|E|}$, where $|E|$ is the number of connected edges of the network, and then the similarity between node i and j in each step can be calculated by the following equation:

$$S_{ij}^{LRW}(t) = \frac{k_i}{2|E|}\pi_{ij}(t) + \frac{k_i}{2|E|}\pi_{ji}(t) \tag{5}$$

However, in the process of wandering from node i to j, the wanderer may gradually move away from node i and j, even if the distance between node i and j is very close. Under the circumstances, the prediction precision may be lowered, because walkers tend to stay in local areas instead of wandering to the rest of the network. So that, we superpose the random walking results of each step. According to literature [16], after each random walk process is superposed, the similarity between nodes will eventually be higher, as shown in Eq. (6).

$$S_{ij}^{SRW}(t) = \sum_{l=1}^{t} S_{ij}^{LRW}(l) \tag{6}$$

where SRW represents superposed random walk.

To sum up, we can calculate the similarity between the Nth node and all the previous $N-1$ nodes by Eq. (6), which is expressed by $S^{SRW} = [S_{1N}, S_{2N}, \dots, S_{(N-1)N}]$. The similarity calculation results in S^{SRW} are sorted from big to small, and they are named as $S_{M_{(1)}N}, S_{M_{(2)}N}, \dots, S_{M_{(N-1)}N}$, and their corresponding nodes $\left(t_{M_{(1)}}, y_{M_{(1)}}\right), \left(t_{M_{(2)}}, y_{M_{(2)}}\right), \dots, \left(t_{M_{(k)}}, y_{M_{(k)}}\right)$ are the top k most similar to the last node (t_N, y_N).

2.3 Construct prediction models

2.3.1 Model 1

Different from reference [16], we consider the first k nodes $\left(t_{M_{(1)}}, y_{M_{(1)}}\right), \left(t_{M_{(2)}}, y_{M_{(2)}}\right), \dots, \left(t_{M_{(k)}}, y_{M_{(k)}}\right)$ that are similar to node (t_N, y_N), and give the following prediction model:

$$y_{N+1} = \sum_{i=1}^{k} \alpha_i \frac{y_{M_{(i)}+1} - y_{M_{(i)}}}{t_{M_{(i)}+1} - t_{M_{(i)}}}(t_{N+1} - t_N) + y_N \tag{7}$$

where $\alpha_i = \frac{S_{M_{(i)}N}}{\sum_{i=1}^{k} S_{M_{(i)}N}}$is the weight. To intuitively show the prediction process of the algorithm put forward in this section, we give a schematic diagram of prediction based on two similar nodes, as shown in Figure 1.

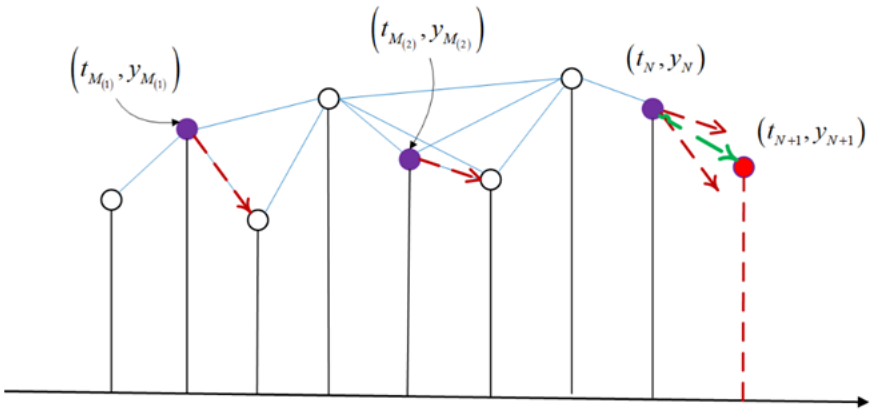

Figure 1: Illustration of Model 1 prediction method with two similar nodes

2.3.2 Model 2

Different from the idea in section 2.3.1, in section 2.2, after we get the top k nodes $\left(t_{M_{(1)}}, y_{M_{(1)}}\right), \left(t_{M_{(2)}}, y_{M_{(2)}}\right), \ldots, \left(t_{M_{(k)}}, y_{M_{(k)}}\right)$ with high similarity with node (t_N, y_N), we weight the trend of the connection between similar nodes and the last node to predict the future nodes, and we can get the following prediction model:

$$y_{N+1} = \sum_{i=1}^{k} \alpha_i \frac{y_N - y_{M_{(i)}}}{t_N - t_{M_{(i)}}} \left(t_{N+1} - t_{M_{(i)}}\right) + y_N \tag{8}$$

where $\alpha_i = \frac{S_{M_{(i)}N}}{\sum_{i=1}^{k} S_{M_{(i)}N}}$ is the weight. To intuitively show the prediction process of the algorithm put forward in this section, we give a schematic diagram of prediction based on two similar nodes, as shown in Figure. 2.

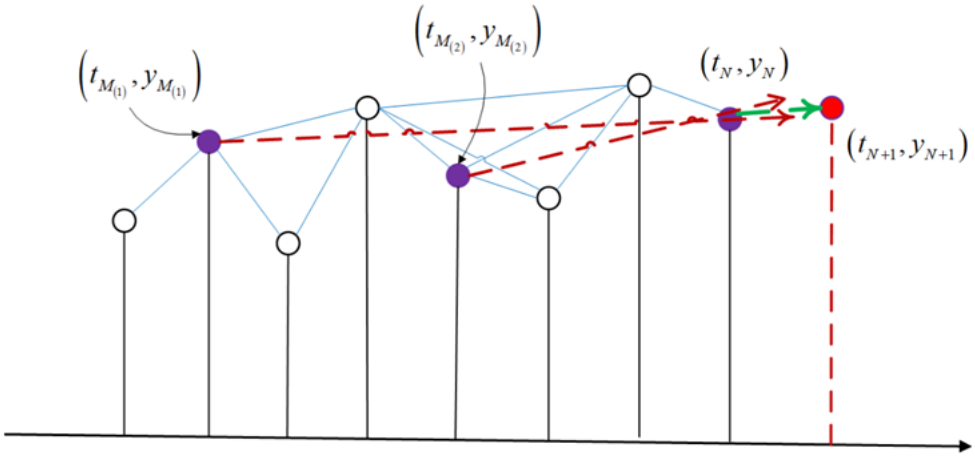

Figure 2: Illustration of Model 2 prediction method with two similar nodes

2.3.3 Combined prediction model

The two types of forecasting models constructed in Section 2.3.1 and 2.3.2 have different emphases. We can roughly divide the change of carbon price into two types: one is to keep a certain trend and change continuously, which can be forecasted by the model in Section 2.3.2; The other is irregular sudden change, which can be forecasted by the model in Section 2.3.1. In order to integrate the advantages of these two models, which can reflect both the sudden change of price and its continuous change, we use the following steps to build a combined forecasting model. Then, we introducing weight parameters

$$\omega_1 = \frac{d_{N \to N+1}}{\sum_{i=1}^{k} d_{M_{(i)} \to N+1}} \tag{9}$$

$$\omega_2 = \frac{\sum_{i=1}^{k} d_{M_{(i)} \to N}}{\sum_{i=1}^{k} d_{M_{(i)} \to N+1}} \tag{10}$$

The combined prediction model can be expressed as

$$\hat{y}_{N+1} = \omega_1 Y_1 + \omega_2 Y_2 \quad (11)$$

where Y_1 is the predicted result of model 1 and Y_2 is the predicted result of model 2.

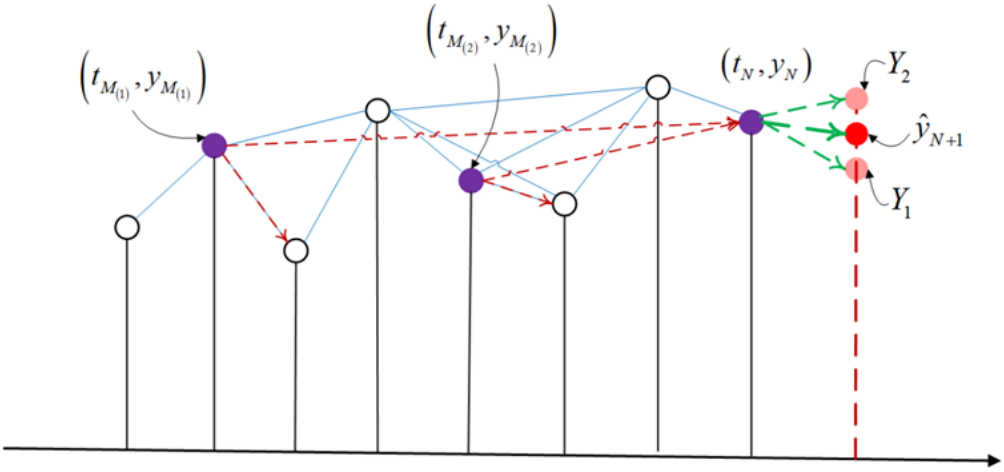

Figure 3: Illustration of the Combined prediction model

2.3.4 Evaluation index of prediction model

To test the prediction effect of the model, we use mean absolute error (MAE), Mean absolute percentage error (MAPE) and Root mean square error (RMSE) as the loss functions to measure the level accuracy,

$$MAE = \frac{1}{N}\sum_{t=1}^{N}|\hat{y}(t) - y(t)|, MAPE = \frac{1}{N}\sum_{t=1}^{N}\frac{|\hat{y}(t)-y(t)|}{y(t)}, \quad (12)$$

$$RMSE = \frac{1}{N}\sqrt{\sum_{t=1}^{N}[\hat{y}(t) - y(t)]^2} \quad (13)$$

where $\hat{y}(t)$ is the estimated value and $y(t)$ the real value.

The directional accuracy of the model can be measured by the following indicator,

$$Dstat = \frac{1}{N}\sum_{t=1}^{N} q_t, \quad q_t = \begin{cases} 1, [y(t+1) - y(t)][\hat{y}(t+1) - y(t)] > 0 \\ 0, otherwise \end{cases} \quad (14)$$

the closer $Dstat$ gets to 1, the more accurate the model is in predicting volatility trends, whereas the closer $Dstat$ gets to 0, the less accurate the model is in predicting volatility trends.

3. Results & Discussion

In research on COVID-19, people tend to focus on two sets of data: the total number of COVID-19 infections in a country or region, and the number of Daily new Cases/confirmed cases in a country or region. In this part, we made prediction and analysis based on the statistics of COVID-19 infections in Pakistan from the perspectives of the total number of infected persons and the daily newly confirmed cases.

3.1 Predictive analysis of total number of COVID-19 infections

In this section, the number of COVID-19 infections in four provinces of Punjab, Balochistan, Isb, and KPK of Pakistan from March 10, 2020 to September 27, 2020 is selected for predictive analysis. The sample data of the four regions are shown in Fig 4 (a-d). It can be seen that from March 10, 2020 to September 27, 2020, the number of COVID-19 infections in four regions showed a trend of rapid growth and then levelling off. When constructing the model for prediction, the data from March 10, 2020 to July 8, 2020 are used as training data to determine the parameters of the model, and the data from July 9, 2020 to September 27, 2020 are used as test data to test the prediction effect of the model.

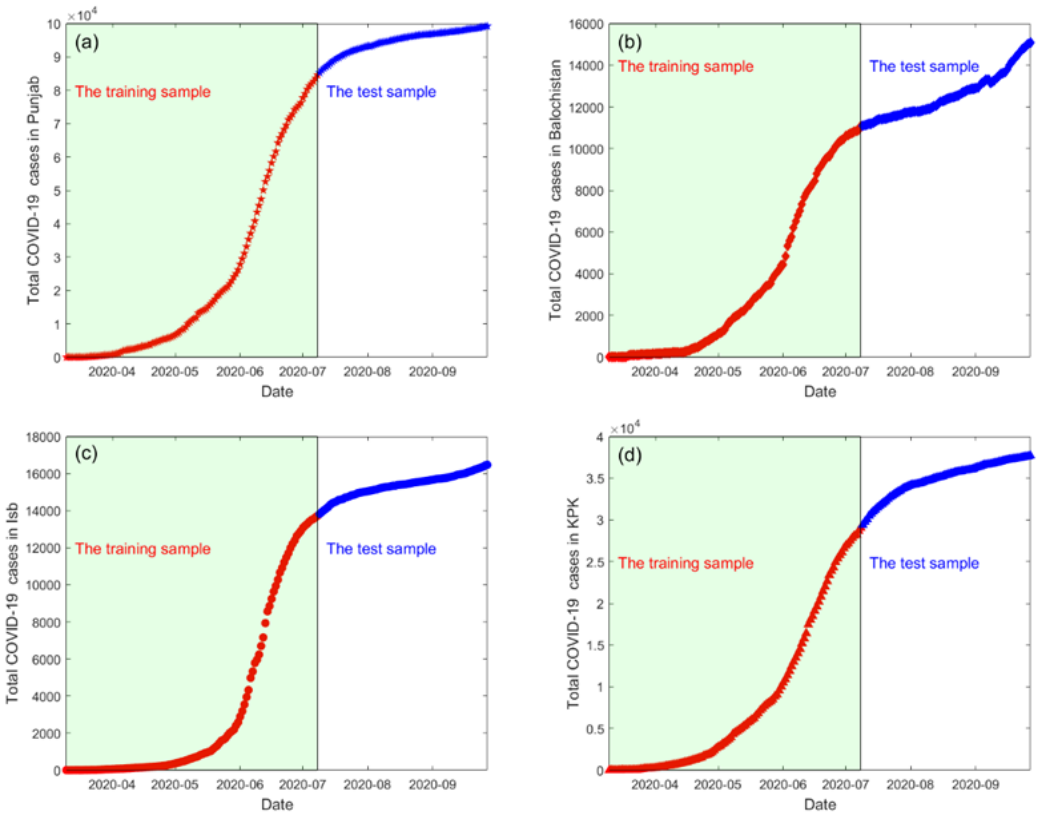

Figure 4: Sample data and training set and test set division, (a) total COVID-19 cases in Punjab, (b) total COVID-19 cases in Balochistan, (c) total COVID-19 cases in Isb, (d) total COVID-19 cases in KPK

According to the model construction method in Section 2.3, the number of similar nodes in the network is an important parameter of the prediction model constructed in this paper. We can build different prediction models according to the different selection of the number of similar nodes in the network. In order to analyze the influence of the number of similar nodes on the prediction accuracy of the model, we selected the number of similar nodes $k = 1,2$ and 3 respectively to construct the prediction models $1-VGLP, 2-VGLP$ and $3-VGLP$ respectively. The three prediction models were used to predict the total number of COVID-19 infections in Punjab, Balochistan, Isb, and KPK. The comparison between the real data and the predicted data in the four regions is shown in Figure 5.

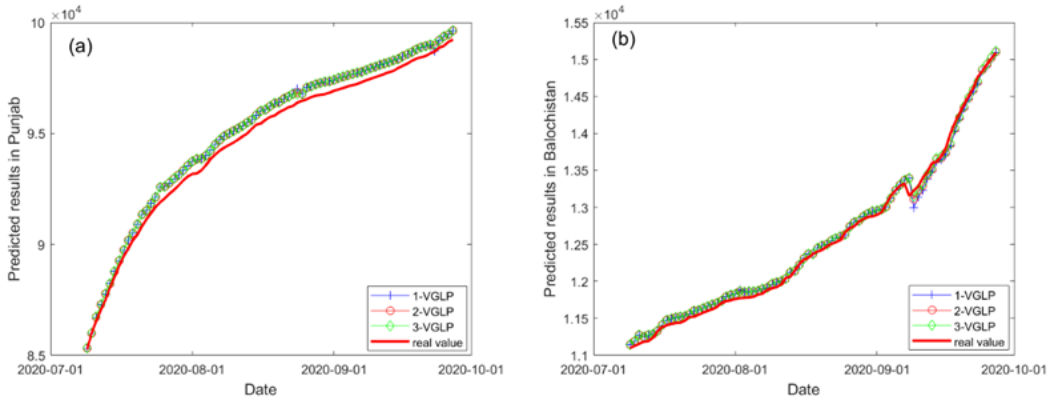

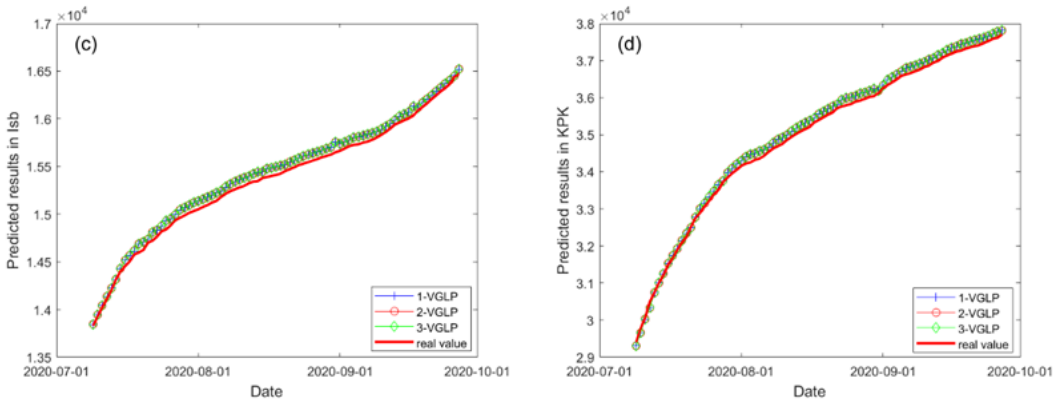

Figure 5: Prediction results of the total number of infected persons in each region, (a) Prediction results of total COVID-19 cases in Punjab, (b) Prediction results of total COVID-19 cases in Balochistan, (c) Prediction results of total COVID-19 cases in Isb, (d) Prediction results of total COVID-19 cases in KPK

As can be seen from Fig. 5, the prediction results of the total number of COVID-19 infections in the four regions based on the prediction model constructed in this paper have a very similar trend to the real data. At the same time, we can also see that the results of the three prediction models, 1-VGLP,2-VGLP and 3-VGLP, are slightly different. In order to accurately analyze the prediction accuracy of the three prediction models $1-VGLP$, $2-VGLP$ and $3-VGLP$, we further calculated the accuracy index of the prediction results of each model, and the results are shown in Table 1.

Table 1: Prediction accuracy of the three prediction models for the total number of infected persons

	Model	MAE	MAPE	RMSE	Dstat
Punjab	$1-VGLP$	435.0978	0.0046	50.2747	1.0000
	$2-VGLP$	437.9378	0.0046	50.2937	1.0000
	$3-VGLP$	440.1000	0.0046	50.4932	1.0000
Balochistan	$1-VGLP$	58.4627	0.0047	8.1335	0.9259
	$2-VGLP$	52.1723	0.0042	6.9561	0.9630
	$3-VGLP$	50.2066	0.0041	6.6887	0.9753
Isb	$1-VGLP$	64.4500	0.0042	7.5712	1.0000
	$2-VGLP$	65.0875	0.0042	7.6372	1.0000
	$3-VGLP$	65.7291	0.0043	7.7037	1.0000
KPK	$1-VGLP$	131.9317	0.0037	15.6156	1.0000
	$2-VGLP$	132.4608	0.0037	15.6774	1.0000
	$3-VGLP$	133.0055	0.0038	15.7412	1.0000

As can be seen from Table 1, from the calculation results of level accuracy indexes (including MAE, MAPE and RMSE), the level accuracy index values of the total number of infected persons in Punjab, Isb and KPK regions increased with the increase of similar nodes, indicating that the level accuracy of the prediction model showed a downward trend. However, the level accuracy index value of the total number of infected people in Balochistan province decreases with the increase of similar nodes, indicating that the level accuracy of the prediction model presents an upward trend. According to the calculation results of the directional accuracy index, the value of the directional accuracy index for the prediction of the total number of infected persons in Punjab, Isb and KPK regions by the three models is 1, indicating that the prediction model is accurate in predicting the change trend of the total number of infected persons in these three regions. In Balochistan, the prediction accuracy index of directivity increases with the increase of similar nodes, indicating that the prediction accuracy of directivity of the model improves. The above results show that the COVID-19 prediction model constructed in this paper based on complex network has high accuracy in predicting the total number of COVID-19 infections. The number of similar nodes selected in the model can affect the prediction accuracy of the model, and the

prediction accuracy of the model can be effectively improved by adjusting the number of similar nodes in the model.

3.2 Predictive analysis of daily new cases of COVID-19

In this part, we forecast the daily new cases of COVID-19 in Balochistan, Isb, KPK and Sindh provinces. Daily new data for Balochistan, Isb and KPK provinces from 10 March 2020 to 26 September 2020 and for Sindh province from 28 April 2020 to 29 September 2020 were selected as sample data. In Balochistan, Isb and KPK provinces, daily new cases from 10 March 2020 to 7 July 2020 were used as training data to construct VG networks. Three prediction models, 1-VGLP,2-VGLP and 3-VGLP, were used to predict the daily new cases from July 8, 2020 to September 26, 2020. In Sindh Province, daily new cases from April 28, 2020 to July 29, 2020 were used as training data to construct VG network, and three prediction models, 1-VGLP,2-VGLP and 3-VGLP, were used to predict daily new cases from July 30, 2020 to September 29, 2020 respectively. The sample data selected in this part is shown in Figure 6.

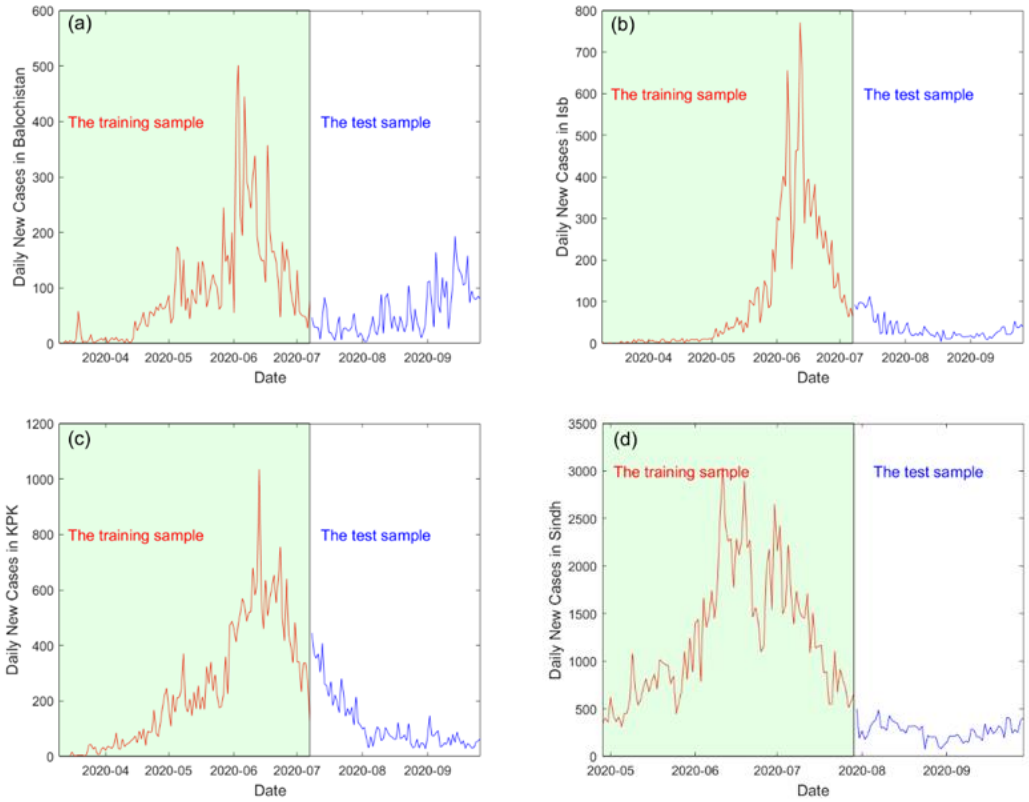

Figure 6: Sample data and division of training set and test set, (a) Daily New Cases in Balochistan, (b) Daily New Cases in Isb, (c) Daily New Cases in PKP, (d) Daily New Cases in Sindh

As can be seen from Figure 6, the daily new cases in the four regions fluctuated greatly, presenting complex nonlinear characteristics. The mean daily new cases in Balochistan, Isb, KPK and Sindh were 76.4925, 79.7164, 188.6965 and 852.4516, respectively. The standard deviations are 82.4419, 127.5705, 190.1669 and 708.7542. As you can see, Sindh has the greatest variation in daily new cases, followed by KPK, and Balochistan has the least variation. Three prediction models, 1-VGLP,2-VGLP and 3-VGLP, were used to predict the daily new cases in the four regions, as shown in Figure. 7

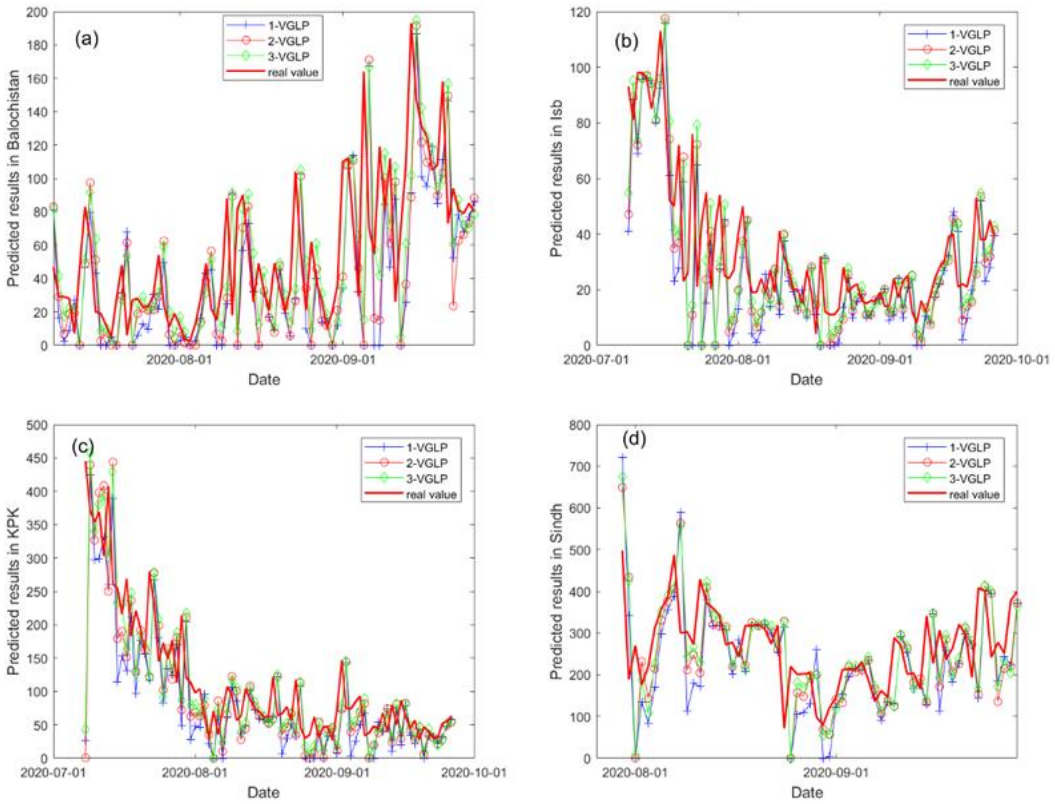

Figure 7: Prediction results of daily new cases in each region, (a) Balochistan, (b) Isb, (c) KPK, (d) Sindh

As can be seen from Figure 7, the COVID-19 prediction model constructed in this paper can better predict the change trend of daily new cases in Balochistan, Isb, KPK and Sindh provinces, and the different number of similar nodes selected in the model will have a certain influence on the prediction results of the model. Further, we calculated the accuracy index results of the three prediction models 1-VGLP,2-VGLP and 3-VGLP for the prediction of daily new cases in the four provinces, as shown in Table 2

Table 2: Prediction accuracy indexes of the three prediction models for the daily new cases

	Model	MAE	MAPE	RMSE	Dstat
Balochistan	$1-VGLP$	31.9006	0.8075	4.9141	0.5185
	$2-VGLP$	31.2945	0.7695	4.8537	0.5695
	$3-VGLP$	30.3900	0.7476	4.6697	0.6312
Isb	$1-VGLP$	15.8193	0.5544	2.3121	0.5065
	$2-VGLP$	14.5923	0.5178	2.1680	0.5595
	$3-VGLP$	14.1347	0.5052	2.1312	0.6295
KPK	$1-VGLP$	52.0991	0.5074	8.5007	0.5185
	$2-VGLP$	49.5198	0.4908	8.4363	0.5745
	$3-VGLP$	44.9664	0.4511	7.7109	0.6452
Sindh	$1-VGLP$	89.7013	0.4024	15.1982	0.5035
	$2-VGLP$	78.8512	0.3485	13.9154	0.5485
	$3-VGLP$	75.4095	0.3377	13.5607	0.6235

As can be seen from Table 2, the value of the level accuracy index of the prediction model decreases with the increase of the number of similar nodes, and the value of the directional accuracy index of the model increases with the increase of the number of similar nodes, indicating that the daily new cases of COVID-19 in Balochistan, Isb, KPK and Sindh provinces are predicted. Both level accuracy and directional accuracy of the prediction model constructed in this paper are improved with the increase of similar nodes selected in the model.

4.Conclusion

This paper proposes a novel COVID-19 prediction method based on a combination of viewable network and link prediction. The basic idea of model construction is to transform COVID-19 data into a complex network using visibility algorithm, and determine node similarity in the network with link prediction method. On the basis of analyzing the similarity of nodes, two initial prediction methods are proposed, that is, the weighted prediction method of similarity node change trend and the weighted prediction method of similarity node trend extrapolation. In order to integrate the advantages of the two prediction methods, we constructed a new COVID-19 prediction model by weighted combination of the two based on the principle of new information priority in the prediction process and distance factor. The numerical simulation results show that the viewable network constructed by us can effectively capture the structural changes of original data. In the empirical part, we get the following main conclusions: The COVID-19 prediction model built in this paper based on complex network has high accuracy in predicting the total number of COVID-19 infections. The number of similar nodes selected in the model can affect the prediction accuracy of the model, and the prediction accuracy of the model can be effectively improved by adjusting the number of similar nodes in the model. Compared with traditional prediction methods, the method proposed in this paper can not only get good prediction results, but also find the previous state similar to the current node state, so as to further analyze the number of COVID-19 infections.

Acknowledgment

This work was supported by the National Key Research and Development Program of China (Grant No. 2020YFA0608602), the National Natural Science Foundation of China (Grant No. 72243005,72174091), Qing Lan Project of Jiangsu Province (2021), Special Science and Technology Innovation Program for Carbon Peak and Carbon Neutralization of Jiangsu Province (Grant No. BE2022612) and the China Postdoctoral Foundation (Grant No. 2021M691312).

References

[1]. Ahmed, S.F.; Quadeer, A.A.; McKay, M.R. Preliminary identification of potential vaccine targets for the COVID-19 coronavirus (SARS-CoV-2) based on SARS-CoV immunological studies. Viruses 2020, 12, 254.

[2]. Lescure, F.-X.; Bouadma, L.; Nguyen, D.; Parisey, M.; Wicky, P.-H.; Behillil, S.; Gaymard, A.; Bouscambert-Duchamp, M.; Donati, F.; Le Hingrat, Q.; et al. Clinical and virological data of the first cases of COVID-19 in Europe: A case series. Lancet Infect. Dis. 2020, 20, 697–706.

[3]. Xu, B.; Gutierrez, B.; Mekaru, S.; Sewalk, K.; Goodwin, L.; Loskill, A.; Cohn, E.L.; Hswen, Y.; Hill, S.C.; Cobo, M.M.; et al. Epidemiological data from the COVID-19 outbreak, real-time case information. Sci. Data 2020, 7, 106.

[4]. Fang, Y.; Zhang, H.; Xie, J.; Lin, M.; Ying, L.; Pang, P.; Ji, W. Sensitivity of chest CT for COVID-19: Comparison to RT-PCR. Radiology 2020.

[5]. Heymann, D.L.; Shindo, N. COVID-19: What is next for public health? Lancet 2020, 395, 542–545.

[6]. Tan, L.; Wang, Q.; Zhang, D.; Ding, J.; Huang, Q.; Tang, Y.-Q.; Wang, Q.; Miao, H. Lymphopenia predicts disease severity of COVID-19: A descriptive and predictive study. Signal Transduct. Target. Ther. 2020, 5, 33.

[7]. Liu, W.; Zhang, Q.; Chen, J.; Xiang, R.; Song, H.; Shu, S.; Chen, L.; Liang, L.; Zhou, J.; You, L.; et al. Detection of COVID-19 in children in early January 2020 in Wuhan, China. N. Engl. J. Med. 2020, 382, 1370–1371.

[8]. Qiu, H.; Wu, J.; Hong, L.; Luo, Y.; Song, Q.; Chen, D. Clinical and epidemiological features of 36 children with coronavirus disease 2019 (COVID-19) in Zhejiang, China: An observational cohort study. Lancet Infect. Dis. 2020, 20, 689–696.

[9]. Bai, Y.; Yao, L.; Wei, T.; Tian, F.; Jin, D.-Y.; Chen, L.; Wang, M. Presumed asymptomatic carrier transmission of COVID-19. JAMA 2020, 323, 1406–1407.

[10]. Barabási A L, Albert R. Emergence of scaling in random networks[J]. science, 1999, 286(5439): 509-512.

[11]. Watts D J, Strogatz S H. Collective dynamics of ‘small-world’networks [J]. nature, 1998, 393(6684): 440-442.
[12]. Newman M E J, Watts D J. Renormalization group analysis of the small-world network model [J]. Physics Letters A, 1999, 263(4-6): 341-346.
[13]. Erdős P, Rényi A. On the existence of a factor of degree one of a connected random graph [J]. Acta Math. Acad. Sci. Hungar, 1966, 17: 359-368.
[14]. Lacasa L, Luque B, Ballesteros F, et al. From time series to complex networks: The visibility graph [J]. Proceedings of the National Academy of Sciences, 2008, 105(13): 4972-4975.
[15]. Luque B, Lacasa L, F Ba llesteros, et al. Horizontal visibility graphs: exact results for random time series. Physical Review E, 2010, 80(4 Pt 2):046103.
[16]. Mao S, Xiao F. A novel method for forecasting construction cost index based on complex network [J]. Physica A: Statistical Mechanics and its Applications, 2019, 527: 121306.